



Article

Effect of Grassland Fires on Dust Storms in Dornod Aimag, Mongolia

Ling Wen ^{1,2,3}, Mei Yong ^{1,2,*} , Yulong Bao ^{1,2}, Rong Fu ⁴ and Eerdemutu Jin ^{1,2}

- ¹ College of Geographical Science, Inner Mongolia Normal University, Hohhot 010022, China; 20214019060@mails.imnu.edu.cn (L.W.); baoyulong@imnu.edu.cn (Y.B.); eerdemutu@imnu.edu.cn (E.J.)
- ² Inner Mongolia Key Laboratory of Remote Sensing & Geography Information System, Inner Mongolia Normal University, Hohhot 010022, China
- ³ Provincial Key Laboratory of Mongolian Plateau's Climate System, Inner Mongolia Normal University, Hohhot 010022, China
- ⁴ Inner Mongolia Autonomous Region Surveying and Mapping Geographic Information Center, Hohhot 010010, China; bfrnmch1012@gmail.com
- * Correspondence: yongmei2012@imnu.edu.cn

Abstract: Grassland fires and dust weather in Mongolia can trigger major cascading disasters. Grassland fires from autumn to the following spring can indirectly affect dust weather occurrence in the spring by affecting land surface vegetation cover. In this paper, we selected the aimag (province) of Dornod, Mongolia, a typical temperate grassland area, as the study area. The study aims to (1) analyze the spatiotemporal patterns of grassland fire and dust weather in the past 22 years, as well as the effect of grassland fire on dust weather and to (2) explore in depth the mechanisms of the effects of grassland fire on dust weather. To achieve these goals, we utilize high-resolution satellite burned-area data and Synop dust data. In general, grassland fire and dust weather occurrence clearly varied spatiotemporally across the study area. Grassland fires are typically more frequent in spring and autumn, and dust weather is mainly concentrated in spring. Cumulative grassland fires (both days and burned area) from autumn to the following spring affected the spring cumulative dust weather days significantly, especially the spring cumulative dust storm days. Analysis of the mechanism of the effect of grassland fire on dust storms showed that abundant summer precipitation resulted in higher vegetation cover and more accumulated fuel from autumn to April of the following spring. Consequently, the cumulative grassland fire days were higher, and the cumulative burned area was larger during the period, leading to a significant increase in cumulative dust storm days in May of the spring. In Mongolia, grassland fires are often caused by human factors. The findings of the present study could facilitate the crafting of measures to prevent and reduce grassland fires and indirectly minimize dust weather frequency to protect the ecological environment and promote sustainable development.

Keywords: grassland fire; dust weather; spatiotemporal variation; Pearson correlation analysis; Dornod aimag



Citation: Wen, L.; Yong, M.; Bao, Y.; Fu, R.; Jin, E. Effect of Grassland Fires on Dust Storms in Dornod Aimag, Mongolia. *Remote Sens.* **2023**, *15*, 5629. <https://doi.org/10.3390/rs15245629>

Academic Editors: Sandra Buján and Diego Di Martire

Received: 29 September 2023

Revised: 26 November 2023

Accepted: 30 November 2023

Published: 5 December 2023



Copyright: © 2023 by the authors. Licensee MDPI, Basel, Switzerland. This article is an open access article distributed under the terms and conditions of the Creative Commons Attribution (CC BY) license (<https://creativecommons.org/licenses/by/4.0/>).

1. Introduction

Temperate grasslands are an essential component of terrestrial ecosystems, and they provide a material basis for animal husbandry development in addition to supporting human survival [1,2]. Fires and dust events in temperate grassland ecosystems have attracted considerable attention from researchers as major natural disasters. Grassland fires arise from combustible materials burning and the fire spreading under favorable conditions following contact with a fire source (mostly caused by human activity in Mongolia), causing varying degrees of damage to grassland [3,4]. Dust weather, conversely, refers to meteorological disasters in which strong winds sweep over deserts or arid surfaces, causing dust to be swept into the air, in turn reducing visibility [5]. Dust weather can be categorized

into floating dust, blowing dust, dust storms, and severe dust storms, based on visibility level [6]. Among them, floating dust and blowing dust are weak dust weather, while dust storms and severe dust storms are strong dust weather [7,8]. Grassland fires and strong dust weather, as sudden-onset disaster phenomena, have substantial impacts on grassland ecosystems, biogeochemical cycles, human life and property, social stability, and economic development due to their high hazard level, wide range, and forecast difficulty [9–13]. Notably, the effects of grassland fires and dust events may be superimposed or mutually reinforcing, leading to additional severe cascading disasters. For example, the occurrence of grassland fires destroys vegetation cover and leaves the ground bare [14,15], which facilitates the occurrence of dust events [16–18]. Furthermore, dust events are typically accompanied by strong winds, which could exacerbate fire formation and spread the smoke and sparks generated by the fires over greater distances, triggering new fires [13]. With the ensuing global climate change, extreme weather events are becoming more frequent [19,20]. Several studies have shown that both grassland fires and dust weather have increased in Mongolia recently [8,21,22]. Therefore, it is crucial to investigate whether grassland fires affect dust weather and the potential underlying mechanisms.

In recent years, researchers have conducted extensive studies on fire and dust weather using various approaches. Some researchers have used fire statistics and satellite burned-area data to analyze the spatiotemporal patterns of fire in different regions [3,4,21,23,24]. Other researchers have studied changes in the Normalized Difference Vegetation Index (NDVI) on land surface before and after fire to determine changes in surface vegetation cover and assess vegetation recovery [14,25,26]. According to the studies, fires directly damage surface vegetation cover. In dust weather studies, researchers have used ground-based dust observation data to analyze the spatiotemporal patterns of dust weather in different regions [8,27–32]. Other researchers have used remote sensing image inversion data and reanalysis information to analyze the factors influencing dust weather in different areas [16,33–36]. Among them, Lee and Sohn [34] calculated the correlation between dust frequency and NDVI in the Mongolian Plateau. Their results demonstrated a significant negative correlation between dust frequency and NDVI. Overall, fires typically damage surface vegetation cover, resulting in a decrease in NDVI. In addition, reduction in NDVI can increase in dust weather frequency. Yu and Ginoux [15] analyzed extreme dust emissions from an area subjected to bushfires in Australia in 2019–2020. They reported that high dust concentrations occurred in burned areas with reduced vegetation cover. However, recent studies have mainly focused on grassland fires or dust events unilaterally, and few studies have analyzed both from a disaster cascade perspective. In addition, the interactions between grassland fires and dust weather have been rarely quantified. Therefore, some uncertainty about the effect of grassland fires on dust weather persists.

Furthermore, the mechanisms by which grassland fires affect dust weather should be elucidated. According to Du et al. [37], abundant summer precipitation in the steppe regions of Mongolia increases vegetation cover in the autumn. Consequently, there is more fuel, such as withered grass, in the autumn to the following spring, leading to more frequent grassland fires. Grassland fires directly burn the surface vegetation and leave the ground bare [14,15], which is conducive to spring dust weather occurrence [16–18]. Understanding the mechanisms of the effects grassland fire on dust weather mentioned above could facilitate the formulation of relevant disaster prevention and mitigation measures in addition to ecological environment protection and sustainable development.

We selected the aimag (province) of Dornod in Mongolia, a typical temperate grassland area, as the study area. High-resolution satellite burned-area data and Synop dust data from 2001 to 2022 are used to (1) analyze the spatiotemporal patterns of grassland fires and dust weather, (2) reveal the lagged effect of grassland fire on dust weather, and (3) explore the underlying mechanisms via which grassland fires influence dust weather.

2. Materials and Methods

2.1. Study Area

Dornod is an eastern-border aimag of Mongolia, bordering the Inner Mongolia Autonomous Region of China to the east and southeast, the Hentii and Sukhbaatar aimags of Mongolia to the west and southwest, and the Outer Baileyer Region of Russia to the north (46°25′–50°28′N; 112°05′–119°56′E). As shown in Figure 1, the study area has four long-term weather stations that compile detailed and comprehensive dust weather observations and meteorological data. The terrain is dominated by high plains and low hills. The mountainous areas in the northern foothills of the Greater Khingan Mountains in the southeast and the Hentii Mountains in the northwest are low hills, whereas the remainder is a high plain. The elevation is approximately 548–1481 m throughout the region (Figure 1). The climate is a typical continental climate with four distinct seasons, including long cold winters and short hot summers. Historical meteorological data show that the average annual temperature is $-2.3\text{ }^{\circ}\text{C}$ – $3.14\text{ }^{\circ}\text{C}$, while the average temperature in January is $-26.39\text{ }^{\circ}\text{C}$ – $-15.52\text{ }^{\circ}\text{C}$ and that in July is $17.92\text{ }^{\circ}\text{C}$ – $23.71\text{ }^{\circ}\text{C}$. The average annual precipitation is 258–306 mm, with 70% concentrated in the summer (June–August). The annual average number of days with strong winds ($>10.8\text{ m/s}$) exceeds 26. Most of the area has typical steppe vegetation, mainly consisting of herbaceous plants such as *Stipa grandis* and *Stipa sareptana* [38]. In addition, a portion of the area contains meadow steppe vegetation, including herbaceous plants such as *Stipa baicalensis* and *Leymus chinensis*, as well as some shrubs [38]. As a result, grassland fires occur frequently because of the high storage of fuel, such as withered grass, coupled with the conducive weather and climatic conditions, such as low average annual temperatures, significant temperature differences, low precipitation, high evaporation, dry climate, and abundant sunlight. Between 2001 and 2022, there was a total of 2022 days of grassland fires in Dornod aimag. Among them, 31 days witnessed large-scale fires (with a burned area exceeding 50,000 ha), with the largest single day covering an expansive area of 352,087.81 ha.

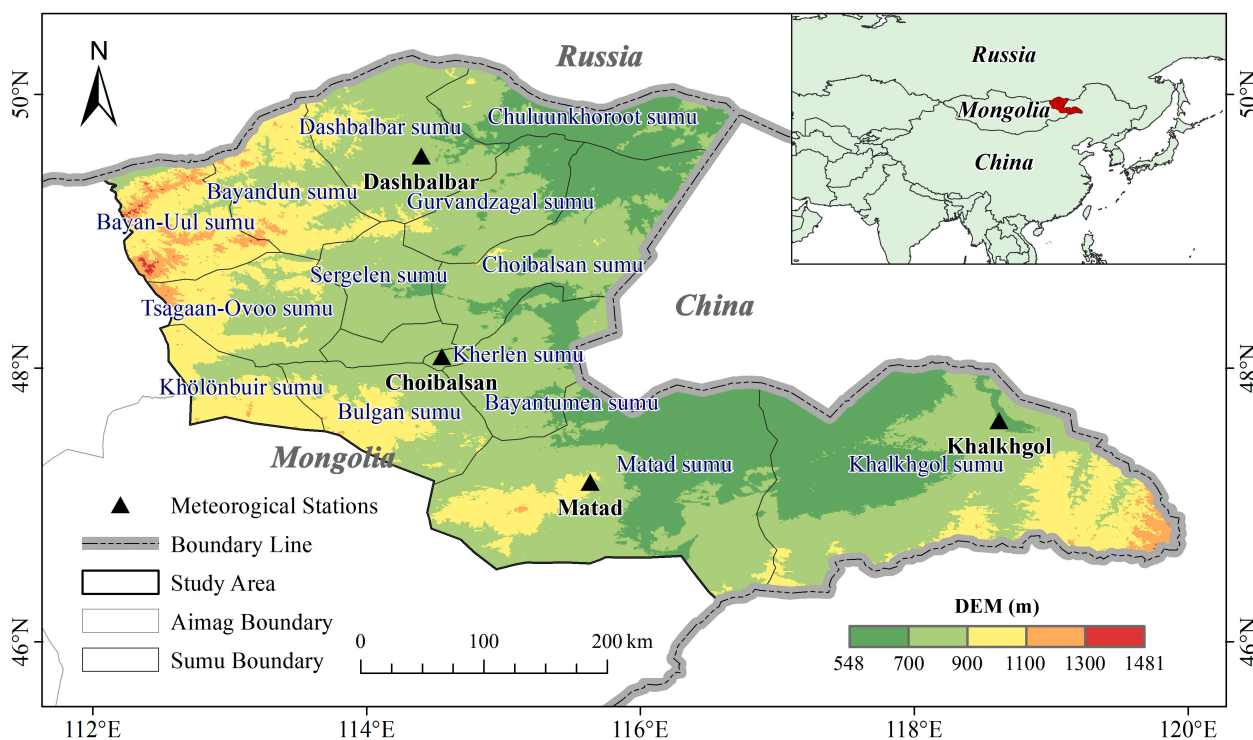


Figure 1. Map of the study area. The background color is the digital elevation model (DEM) of Dornod aimag.

2.2. Data Sources

2.2.1. MCD64A1 Burned-Area Data

Grassland fire data were obtained from the National Aeronautics and Space Administration (NASA) MODIS MCD64A1 burned-area data (<https://ladsweb.modaps.eosdis.nasa.gov/>, accessed on 23 December 2022). It is monthly data with a resolution of 500 m. In the MCD64A1 burn date layer data, “−1” indicates missing, “−2” indicates water, “0” indicates unburned, and “1–366” indicates burn dates [39].

2.2.2. SYNOP Dust Data

The dust weather data were obtained from Surface Synoptic Observations (SYNOP) data (<https://www.ncei.noaa.gov/>, accessed on 1 April 2023). It is reported every 3 h or 6 h, using the weather code (ww) as a two-digit number from 00 to 99 [7,8]. Among them, 06–09, 30–35, and 98 are the codes related to dust weather, and the data were subjected to strict quality control and accuracy tests. Specifically, ww = 06 indicates the occurrence of floating dust, ww = 07 and ww = 08 indicate the occurrence of blowing dust, ww = 09, ww = 30–32, and ww = 98 indicate the occurrence of dust storms, and ww = 33–35 indicate the occurrence of severe dust storms [34,40,41]. Severe dust storms were categorized as dust storms in this paper.

2.2.3. Auxiliary Data

We analyzed the mechanisms by which grassland fires affect dust weather using the NDVI, precipitation, and wind vector data as auxiliary data. NDVI data were obtained from the NASA MODIS MOD13A3 vegetation index product, which is monthly data with a spatial resolution of 1 km. Precipitation and wind vectors were derived from the ERA5 reanalysis dataset published by the European Centre for Medium Weather Forecasting (<https://cds.climate.copernicus.eu/>, accessed on 12 May 2023). Its spatial resolution is $0.25^\circ \times 0.25^\circ$.

2.3. Methods

2.3.1. Statistics of Grassland Fire Days, Burned Area, and Frequency Based on MCD64A1 Burned-Area Data

Figure 2 is a schematic of the study methodology. The Conversion Tools of ArcGIS 10.8 (ESRI, Redlands, CA, USA) and PivotTable in MS Excel (Microsoft Corp., Redmond, WA, USA) were used to count the grassland fire days and burned area. First, the MCD64A1 burn date raster data were converted into polygon data, and the burn date data of “1~366” were extracted from them. Subsequently, the extracted polygon data were exported to an MS Excel file, and the grassland fire days and burned area per month, season, and year from 2001 to 2022 were counted using a PivotTable. The Raster Calculator and Reclassify functions in the Spatial Analyst Tools of ArcGIS 10.8 (ESRI) were used to analyze grassland fire frequency. First, the MCD64A1 burn date raster data were reclassified by reclassifying “−1” and “−2” as “0” and reclassifying “1~366” as “1”. Subsequently, the spatial distribution of grassland fire frequency was obtained by summation with a Raster Calculator.

2.3.2. Dust Weather Days Statistics Based on SYNOP Data

An MS Excel (Microsoft Corp.) PivotTable was used to count the dust weather days in the study area (Figure 2). First, 22 years of data were combined in an MS Excel file, and data with weather codes (ww) of 06 to 09, 30 to 35, and 98 were screened out. Afterward, PivotTables were used to count the number of floating dust days, blowing dust days, dust storm days, and total dust weather days per month, season, and year from 2001 to 2022 at the four stations. If 1 to 3 of the three types of weather, namely floating dust, blowing dust, and dust storms, occurred in a day, we categorized it as a total dust weather day.

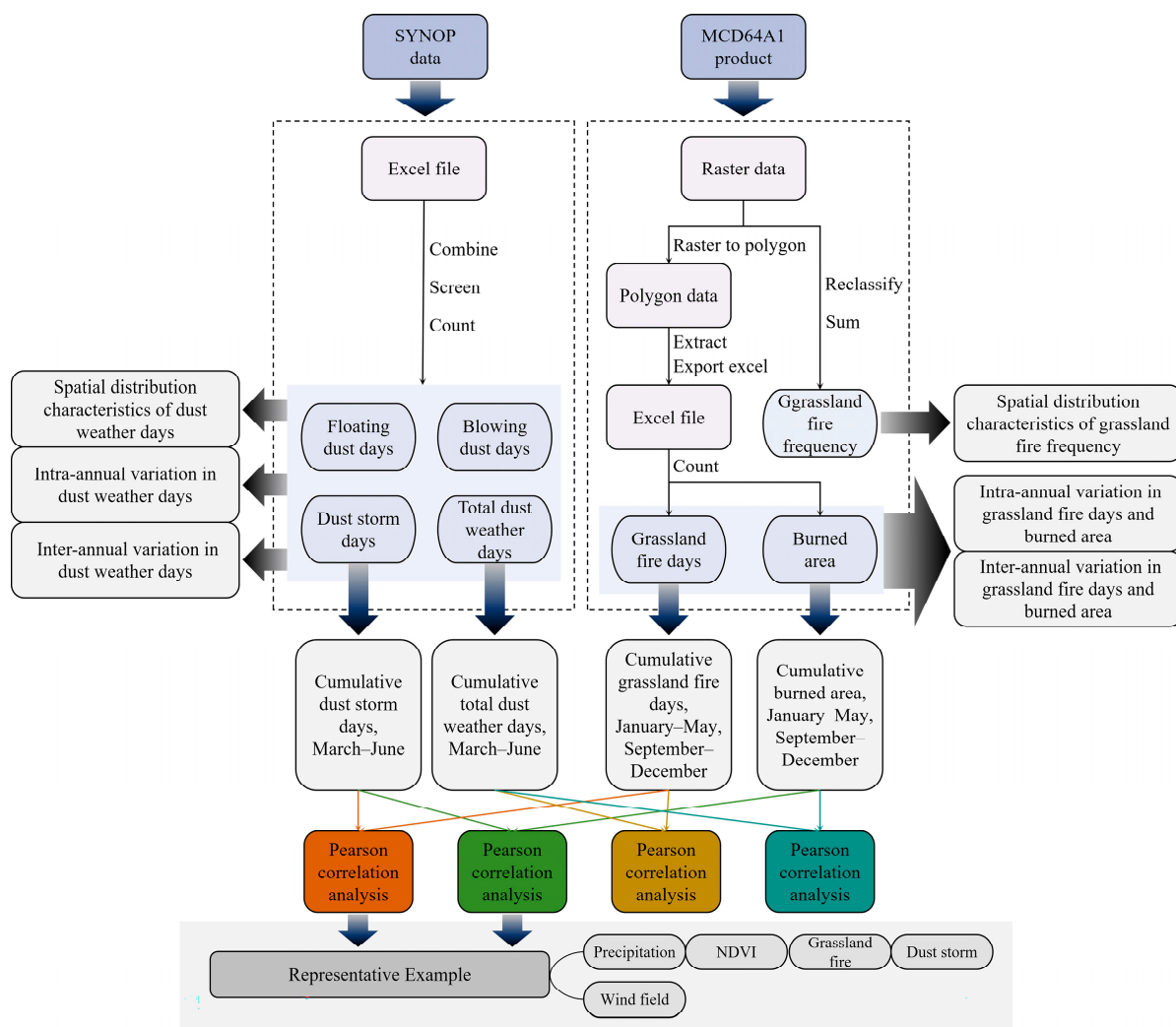


Figure 2. The technical route of the study.

2.3.3. Analysis of Effect of Grassland Fire on Dust Weather

Under arid climatic conditions, grassland vegetation burned by fires in autumn to the following spring cannot be restored quickly, thereby affecting the spring dust weather. Therefore, grassland fire days and burned area data from January to May and from September to December were selected for each year, along with dust weather days (including dust storms and total dust weather) from March to June from 2001 to 2022 and combined into four datasets (Table 1). The dust weather days in the study area were derived by combining data from the four stations and removing duplicates. Finally, Pearson correlation analysis was performed on the four datasets (Figure 2). The formula is as follows:

$$r = \frac{\sum_{i=1}^n (x_i - \bar{x})(y_i - \bar{y})}{\sqrt{\sum_{i=1}^n (x_i - \bar{x})^2 \sum_{i=1}^n (y_i - \bar{y})^2}} \tag{1}$$

where x_i and y_i are the values of variables x and y , respectively. \bar{x} and \bar{y} are the mean values of variables x and y , respectively. Subsequently, we selected a representative set of data from the correlation analysis data and conducted a detailed investigation into the mechanisms by which grassland fires affect dust weather. This analysis encompassed aspects such as precipitation, vegetation cover, time series of grassland fires and dust storms, and wind speed conditions.

Table 1. Example of analyzed data.

Variable <i>x</i>	Variable <i>y</i>
Cumulative grassland fire days (cumulative burned area), September 2001–February 2002	Cumulative total dust weather days (cumulative dust storm days), March 2002
Cumulative grassland fire days (cumulative burned area), September 2001–March 2002	Cumulative total dust weather days (cumulative dust storm days), March–April 2002
Cumulative grassland fire days (cumulative burned area), September 2001–April 2002	Cumulative total dust weather days (cumulative dust storm days), March–May 2002
Cumulative grassland fire days (cumulative burned area), September 2001–May 2002	Cumulative total dust weather days (cumulative dust storm days), March–June 2002
⋮	⋮
Cumulative grassland fire days (cumulative burned area), September 2021–May 2022	Cumulative total dust weather days (cumulative dust storm days), March–June 2022

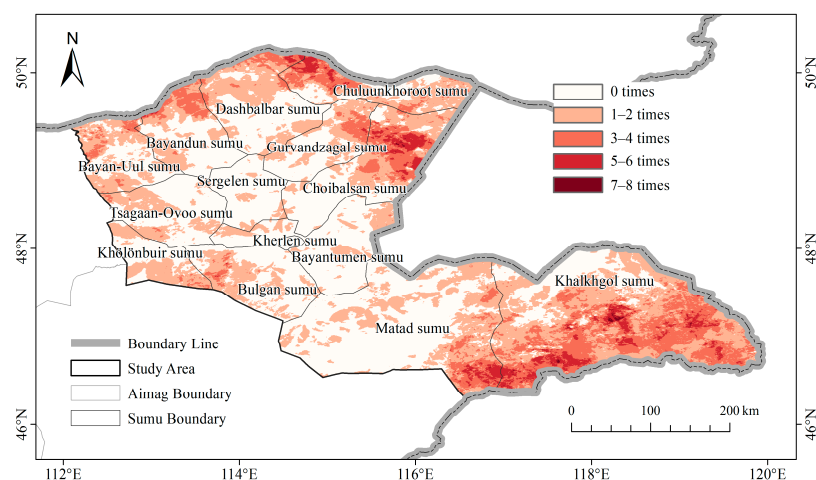
3. Results

3.1. Spatiotemporal Characteristics of Grassland Fires

3.1.1. Spatial Distribution of Grassland Fire Frequency

The present study analyzed the spatial distribution characteristics of grassland fire frequency using NASA MODIS MCD64A1 burned-area data from 2001 to 2022.

As shown in Figure 3, all 14 sumu (administrative divisions) in the study area had at least 1–2 grassland fires. The frequency of grassland fires in the northern part of Bayan-Uul sumu, the northern part of Bayandun sumu, the northwestern part of Tsagaan Ovoo sumu, and the southeastern part of Khölönbuir sumu reached a maximum of 3–4. The frequency of grassland fires in the northeastern part of Dashbalbar sumu, the northwestern part of Chuluunkhoroot sumu, and the western part of Bulgan sumu reached a maximum of 5–6. The frequency of grassland fires in the northern part of Choibalsan sumu, the southern part of Khalkhgal sumu, and the southeastern part of Matad sumu reached a maximum of 7–8. Among them, the area with 7–8 fires was small. On the whole, grassland fires in Dornod aimag occurred mainly in the border areas of northern Bayandun sumu, northwestern Chuluunkhoroot sumu, northern Choibalsan sumu, southern Khalkhgal sumu, and southeastern Matad sumu. Overall, there were more fires in the east than in the west.

**Figure 3.** Spatial distribution of grassland fire frequency in Dornod aimag from 2001 to 2022.

3.1.2. Intra-Annual Variation in Grassland Fire Days and Burned Area

To investigate the intra-annual variation in grassland fires in the study area, we analyzed the monthly and seasonal variation characteristics of grassland fire days and burned area.

As shown in Figure 4a, the monthly variation in grassland fire days and burned area typically followed a saddle-shaped curve. The grassland fire days were higher in April–June and September–October, at 14.09, 14.32, 12.32, 12.59, and 13 days, respectively. The burned area was larger in April–June and October, at 17.66×10^4 ha, 14.33×10^4 ha, 13.35×10^4 ha, and 9.09×10^4 ha, respectively.

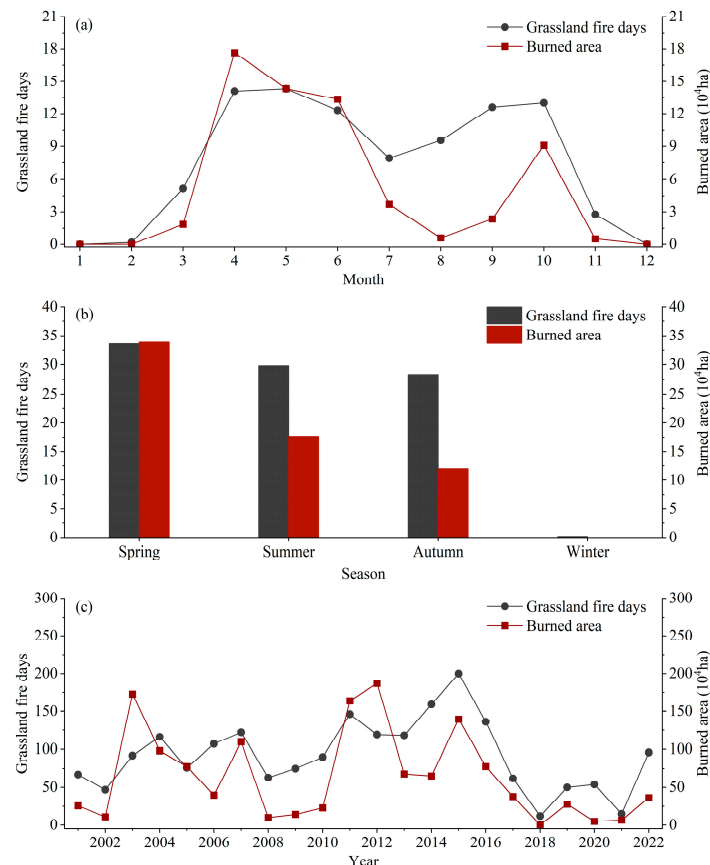


Figure 4. Temporal variations in grassland fire days and burned area in Dornod aimag from 2001 to 2022. (a) Monthly variation; (b) seasonal variation; (c) inter-annual variation.

As shown in Figure 4b, on a seasonal scale, grassland fires were the most frequent in spring, with 33.59 grassland fire days and a burned area of 33.85×10^4 ha, followed by summer (29.77 d and 17.65×10^4 ha) and autumn (28.36 d and 11.97×10^4 ha), while there were almost no fires in winter. In summary, grassland fires occurred at high rates in spring (April to May), summer (June), and autumn (October).

3.1.3. Inter-Annual Variation in Grassland Fire Days and Burned Area

To investigate the inter-annual variation in grassland fires in the study area, we analyzed the inter-annual variation in grassland fire days and burned area.

As shown in Figure 4c, the total number of grassland fire days between 2001 and 2022 was 2222, with an annual average of 91.91 d; and the total burned area was 1396.54×10^4 ha, with an annual average of 63.48×10^4 ha. During the 22-year study period, the grassland fire days were greater in 2007, 2011, and 2014–2016 and reached a peak of 200 d in 2015, followed by a decreasing trend. The burned area was larger in 2003, 2007, 2011–2012, and 2015, and peaked at 186.91×10^4 ha in 2012, followed by a decreasing trend. In

addition, there were apparent alternating increases and decreases in grassland fire days and burned area.

3.2. Spatiotemporal Variation Characteristics of Dust Weather

3.2.1. Spatial Distribution Characteristics of Dust Weather Days

The present study analyzed the spatial distribution characteristics of floating dust days, blowing dust days, dust storm days, and total dust weather days separately using the SYNOP dust data from 2001 to 2022 with annual average dust weather days as an indicator.

As shown in Figure 5, there were relatively few floating dust days in the study area, with no station having more than 0.5 d of floating dust. In contrast, there were more blowing dust days, dust storm days, and total dust weather days at each station, mainly at Choibalsan and Khalkhgol. Specifically, Choibalsan station had the highest number of blowing dust days, whereas Khalkhgol station had the most dust storm days and total dust weather days. Overall, Choibalsan and Khalkhgol stations had a greater number of dust weather days, while Dashblbar and Matad stations had fewer.

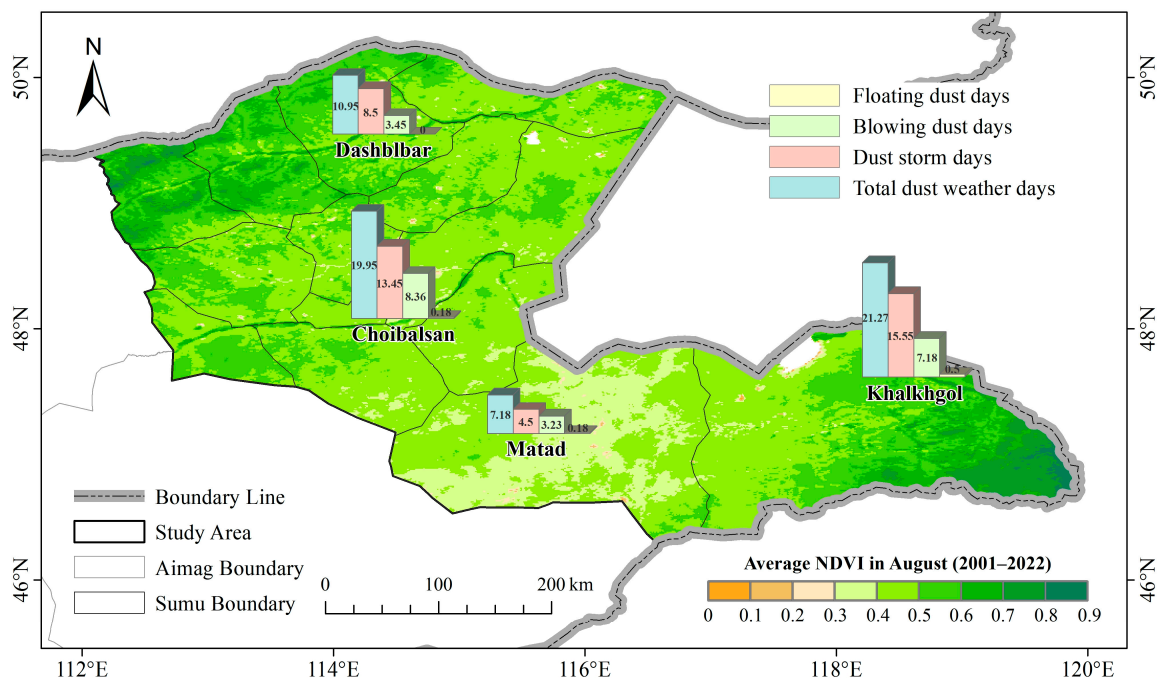


Figure 5. Spatial distribution of dust weather days in Dornod aimag from 2001 to 2022.

3.2.2. Intra-Annual Variation in Dust Weather Days

To investigate the intra-annual variation in dust weather in the study area, we analyzed the monthly and seasonal variation in floating dust days, blowing dust days, dust storm days, and total dust weather days.

As shown in Figure 6a, there were relatively few floating dust days at the four stations, occurring mainly from March to May and in July. In contrast, there were more blowing dust days, dust storm days, and total dust weather days. These were mainly concentrated from March to May, with the highest number in April (Figure 6b–e).

As shown in Figure 7a, the floating dust days at Khalkhgol and Choibalsan stations occurred mainly in spring, whereas the floating dust days at Matad station occurred primarily in summer. Comparatively, each station's blowing dust days, dust storm days, and total dust weather days were mainly concentrated in the spring (Figure 7b–d). In general, dust weather days in the study area were primarily concentrated in spring, followed by autumn, with few occurrences in summer and winter (Figure 6e).

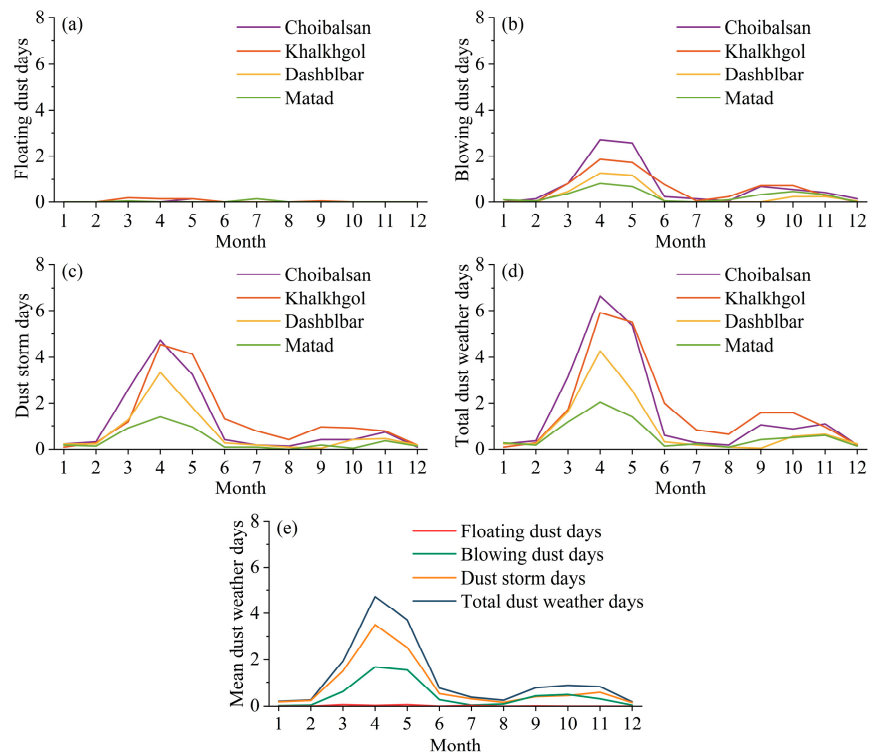


Figure 6. Monthly variations in dust weather days in Dornod aimag from 2001 to 2022. (a) Floating dust days; (b) blowing dust days; (c) dust storm days; (d) total dust weather days; (e) mean dust weather days.

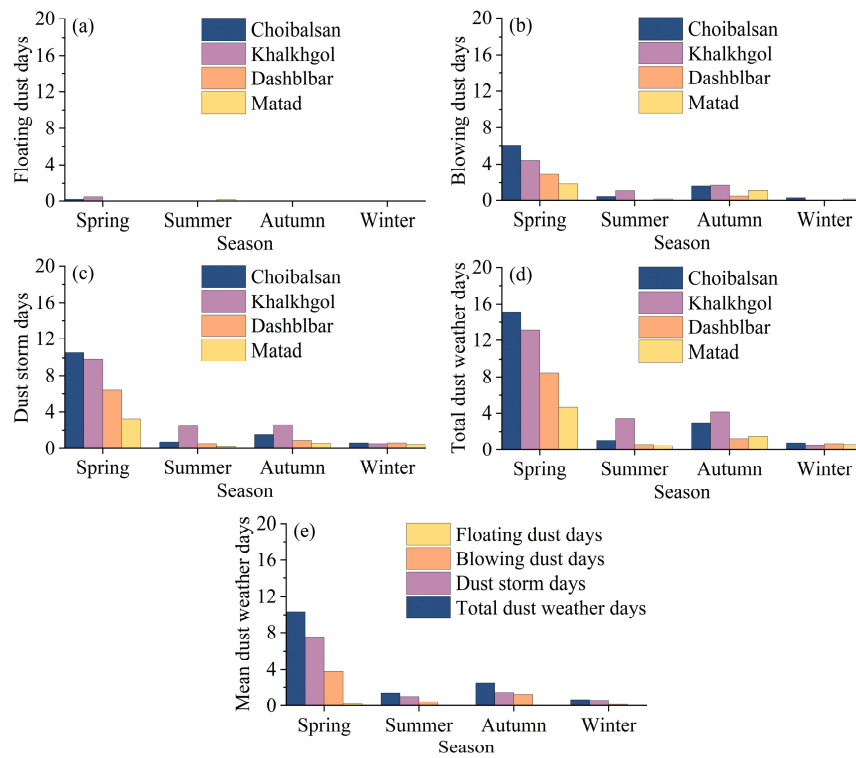


Figure 7. Seasonal variations in dust weather days in Dornod aimag from 2001 to 2022. (a) Floating dust days; (b) blowing dust days; (c) dust storm days; (d) total dust weather days; (e) mean dust weather days.

3.2.3. Inter-Annual Variation in Dust Weather Days

To investigate the inter-annual variation in dust weather in the study area, we analyzed the inter-annual variation characteristics of floating dust days, blowing dust days, dust storm days, and total dust weather days.

As shown in Figure 8a–d, the dust weather in the study area from 2001 to 2022 was dominated by blowing dust and dust storms, and floating dust weather rarely occurred. As shown in Figure 8e, blowing dust days in the study area during the 22-year study occurred more frequently in 2011–2012 and 2019–2022 and reached a peak of 20.5 d in 2020, followed by a decreasing trend. The dust storm days and total dust weather days were more frequent in 2015–2019 and reached peaks of 24 d and 32.25 d, respectively, in 2019. Subsequently, they all showed a decreasing trend, which may have been due to the relatively low grassland fires in the later years of the study (Figure 4c).

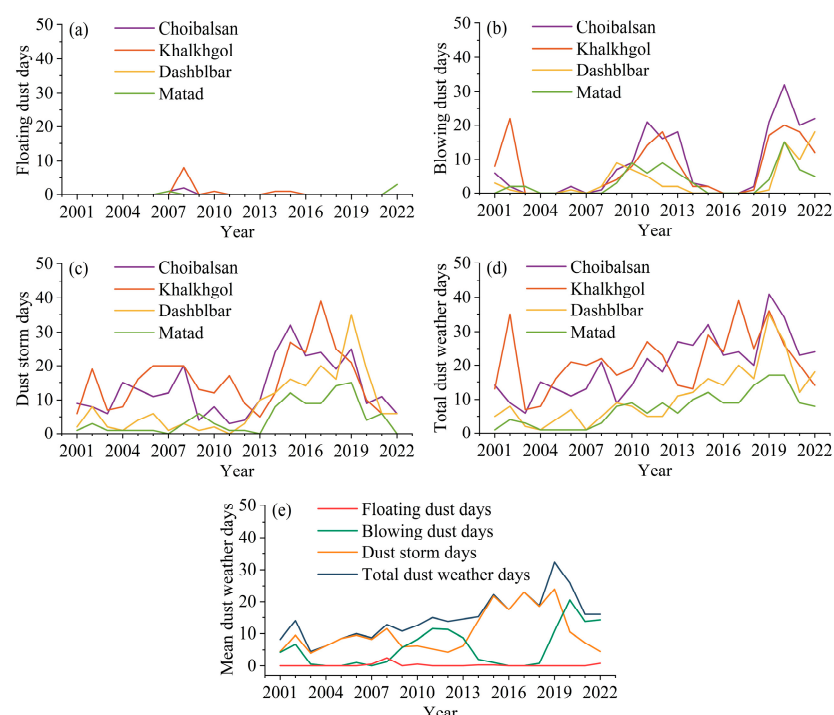


Figure 8. Inter-annual variations in dust weather days in Dornod aimag from 2001 to 2022. (a) Floating dust days; (b) blowing dust days; (c) dust storm days; (d) total dust weather days; (e) mean dust weather days.

3.3. Effects of Grassland Fires on Dust Weather

3.3.1. Effects of Grassland Fires on Total Dust Weather

To explore the effects of grassland fires on total dust weather, the correlations between autumn to the following spring cumulative grassland fires (days and burned area) and the spring cumulative total dust weather days were analyzed.

The results (Table A1 and Figure 9) show that the correlation coefficient between autumn to the following spring cumulative grassland fire days and the spring cumulative total dust weather days was 0.356 ($R^2 = 0.127$; $p > 0$; $n = 81$); the correlation coefficient between autumn to the following spring cumulative burned area and the spring cumulative total dust weather days was 0.295 ($R^2 = 0.0868$; $p > 0$; $n = 79$), and all were positively correlated at the 0.01 level. In contrast, the correlations between autumn to the following spring cumulative grassland fire days and the spring cumulative total dust weather days were stronger.

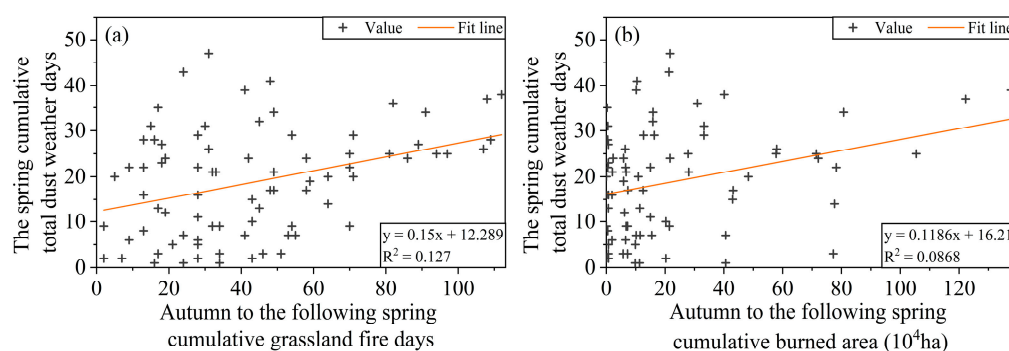


Figure 9. Linear regressions of grassland fire and total dust weather. (a) Linear regression of autumn to the following spring cumulative grassland fire days and the spring cumulative total dust weather days; (b) linear regression of autumn to the following spring cumulative burned area and the spring cumulative total dust weather days. (Note: autumn to the following spring cumulative grassland fire days and burned area are accumulated from September to February/March/April/May of the following year; the spring cumulative total dust weather days are accumulated from March to March/April/May/June).

3.3.2. Effects of Grassland Fires on Dust Storms

To explore the effects of grassland fires on dust storms, the correlations between autumn to the following spring cumulative grassland fires (days and burned area) and the spring cumulative dust storm days were analyzed.

The results (Table A1 and Figure 10) show that the correlation coefficient between autumn to the following spring cumulative grassland fire days and the spring cumulative dust storm days was 0.376 ($R^2 = 0.1414$; $p > 0$; $n = 81$); the correlation coefficient between autumn to the following spring cumulative burned area and the spring cumulative dust storm days was 0.353 ($R^2 = 0.1246$; $p > 0$; $n = 79$), and all were positively correlated at 0.01 level. In contrast, the correlation between autumn to the following spring cumulative grassland fire days and the spring cumulative dust storm days was stronger, which was consistent with that of the spring cumulative total dust weather days. In addition, the significance of the correlation between autumn to the following spring cumulative grassland fire (both days and burned area) and the spring cumulative dust storm days ($p = 0.0005$ and 0.001) was greater than that of the spring cumulative total dust weather days ($p = 0.001$ and 0.008).

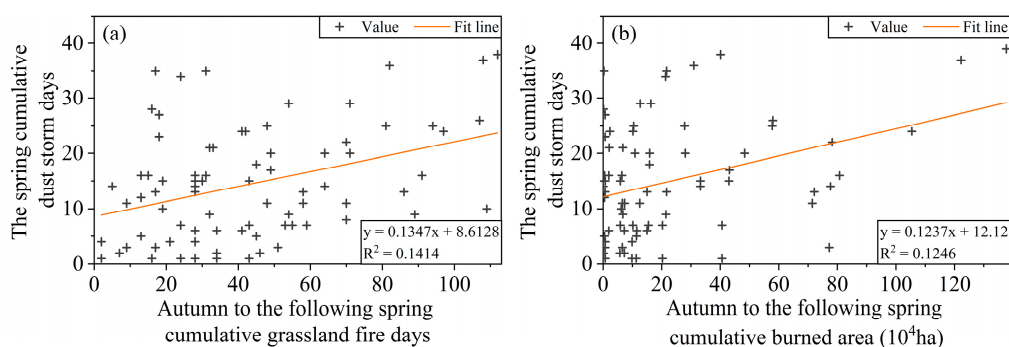


Figure 10. Linear regressions of grassland fire and dust storm. (a) Linear regression of autumn to the following spring cumulative grassland fire days and the spring cumulative dust storm days; (b) linear regression of autumn to the following spring cumulative burned area and the spring cumulative dust storm days. (Note: autumn to the following spring cumulative grassland fire days and burned area are accumulated from September to February/March/April/May of the following year; the spring cumulative dust storm days are accumulated from March to March/April/May/June).

3.4. Analysis of the Mechanisms of the Effects of Grassland Fires on Dust Storms

Based on the analyses in Section 3.3, we selected cumulative grassland fire days and burned area from September 2014 to April 2015, along with cumulative dust storm days from March to May 2015, as representative examples to explore the mechanism by which grassland fires affect dust weather in detail.

As shown in Figure 11a, summer precipitation (June to August) was more abundant in Dornod aimag in 2014 and was above the multiyear average. For the steppe region of Mongolia, the lagging effect of vegetation coverage in autumn on summer precipitation was more significant [37]. As a result, the NDVI was relatively high in autumn 2014 (September to November), and it continued to be high until April 2015 (Figure 11b). Thus, the large amount of withered grass that accumulated during autumn and winter provided a rich fuel source for the occurrence of grassland fires. In addition, persistent drought conditions in the autumn and winter of 2014 and the early spring of 2015 further exacerbated the fire risk (Figure 11a). Under these favorable conditions, the cumulative grassland fire days and burned area between September 2014 and April 2015 reached 108 d and 12.22×10^5 ha, respectively (Figure 11c,d). This was 1.92 times and 2.92 times higher than the annual averages, respectively. Consequently, the vegetation cover decreased over a large area and the soil surface became exposed. This led to 37 cumulative dust storm days between March and May 2015, which was 2.19 times higher than the multiyear average (Figure 11e).

However, the causes of dust storms are complex and there are numerous influencing factors and interactions among the factors [31]. Wind speed is considered the main factor driving dust storms [31]. Therefore, it is necessary to conduct further research from a wind speed aspect. As shown in Table 2 and Figure 12, the cumulative grassland fire days and burned area were the highest from September 2014 to April 2015, resulting in significantly lower vegetation cover in May 2015. In addition, wind speeds were similar in May 2005 and May 2015, and higher in May 2017 and May 2021 than in May 2015 (Figure 12). Under such wind speed conditions, the cumulative dust storm days in March to May 2015 were still greater than those in March to May 2005, 2017, and 2021 (Figure 12). Among them, the cumulative dust storm days in May 2017 at Khalkhgol station were equal to those in May 2015, which could be attributed to the greater wind speed in May 2017. The results of the analysis further indicate that grassland fires affect dust storms indirectly by reducing vegetation cover.

Table 2. Cumulative grassland fire days and burned area.

	Cumulative Grassland Fire Days	Cumulative Burned Area (10^5 ha)
September 2004 to April 2005	33	0.2
September 2014 to April 2015	108	12.22
September 2016 to April 2017	16	0.01
September 2020 to April 2021	13	0.05

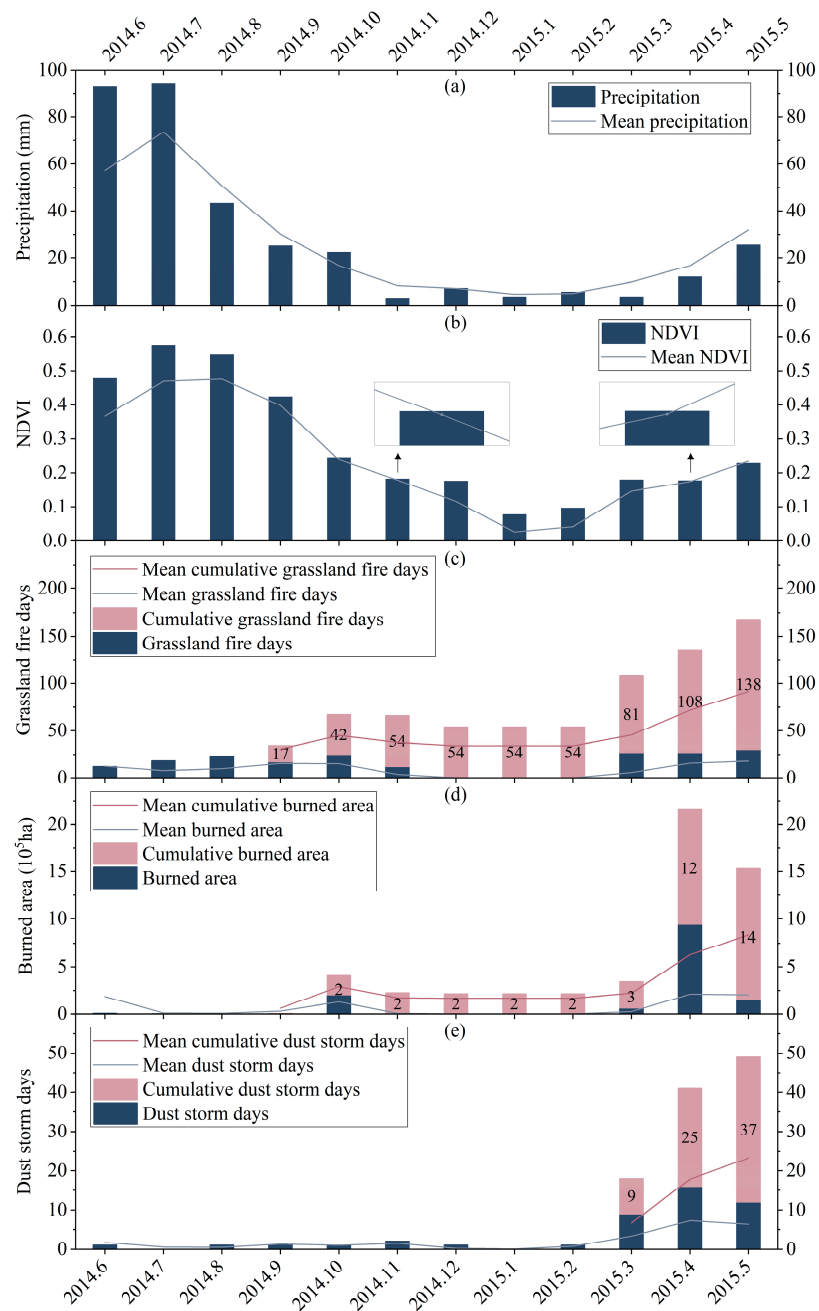


Figure 11. Time series plot for June 2014 to May 2015. The June to December average value (including precipitation, NDVI, grassland fire days, burned area, and dust storm days) is from 2001 to 2014. The January to May average value (including precipitation, NDVI, grassland fire days, burned area, and dust storm days) is from 2001 to 2015. (a) Precipitation; (b) NDVI; (c) grassland fire days; (d) burned area; (e) dust storm days.

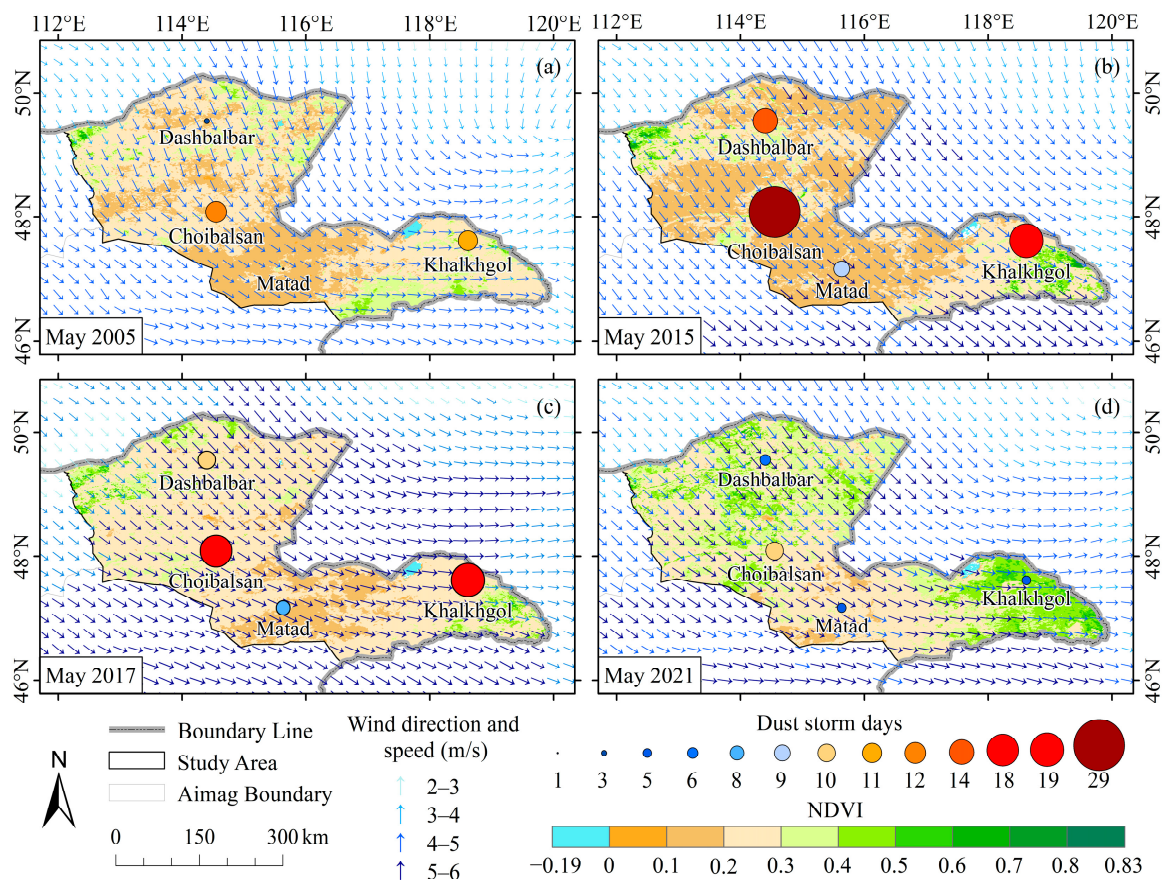


Figure 12. Map of cumulative dust storm days and wind field. The background is NDVI. (a) May 2005; (b) May 2015; (c) May 2017; (d) May 2021. (Note: the wind wind field and NDVI are for May, while the cumulative dust storm days are accumulated from March to May).

4. Discussion

We counted grassland fire days and burned area using MCD64A1 burned-area data, and determined the frequency of grassland fires. Additionally, we analyzed the spatiotemporal characteristics of grassland fires in Dornod aimag. There was apparent spatial heterogeneity in grassland fires in Dornod aimag, and the higher frequency areas were mainly concentrated in regions bordering Russia and China, consistent with the results of the majority of previous research [4,21]. Most of the areas are meadow steppe and have high fuel reserves due to vegetation growing taller and thicker [42], and species renewal and biomass increase faster after fires [43], favoring fire recurrence. Furthermore, the areas are sparsely populated, lack firefighting teams, and are relatively underdeveloped in firefighting technology [21,44]. Therefore, the frequency of grassland fires was higher in the areas. Regarding intra-annual variation, grassland fires occurred at a high rate in spring (April to May), summer (June), and autumn (October). In early spring (late March to early April), snow begins to melt, high temperatures and windy days increase, human activity increases, and grassland fires become more frequent [3]. In contrast, summer (June–August) is characterized by relatively high precipitation and is less prone to fires. However, frequent lightning storms and human activity have led to fires in June [3]. In addition, due to the nomadic lifestyle in Mongolia, pasture vegetation is not harvested in autumn, and the large amount of withered grass leads to more frequent fires in the following spring [44]. In terms of inter-annual variation, the grassland fire days and burned area in the study area have decreased since 2015, which may be related to the increased surface fuel water content due to permafrost thawing in the region [44]. In addition, fuel reserves play an essential role in grassland fires, which are likely to occur when grassland fuel accumulates to a certain level [4,21]. Immediately after a fire, there is a substantial reduction in fuel,

leading to relative fire absence [4,21]. Therefore, there were apparent alternating increases and decreases in grassland fire days and burned area in the study area.

Dust weather days were counted based on the SYNOP dust data and the spatial and temporal characteristics in Dornod aimag were observed. Dust weather was mainly concentrated at the Choibalsan and Khalkhgol stations, potentially due to differences in land use patterns. Mineral resources near Choibalsan station are relatively abundant [45], while a large area of farmland is distributed near Khalkhgol station [43]. Large-scale mining activities and extensive crop cultivation have resulted in damage to surface vegetation and soil loosening, contributing to the occurrence of dust to some extent [46,47]. In addition, the frequent occurrence of grassland fires near Khalkhgol station may be one of the reasons for the greater number of dust weather days at the station. Regarding intra-annual variation, the dust weather days were mainly concentrated in spring (March–May), with the highest number in April [8,31,48]. It may be due to the frequent occurrence of grassland fires in autumn and spring, coupled with drought and low rainfall in the spring, low vegetation cover, large areas of bare ground, rapidly rising temperatures, and large numbers of cold air masses moving southward, which increases the barometric pressure gradient and is conducive to the occurrence of dust weather [8,27,31,34]. Moreover, there were apparent inter-annual variations in the dust weather days in the study area, which may have been the result of a combination of meteorological factors (such as wind speed, temperature, and precipitation), underlying surface factors (such as soil moisture and vegetation cover), and human factors (such as land use practices) [8,16,31,34].

The effect of grassland fire on dust weather was analyzed using the above statistics of grassland fire days and burned area, total dust weather days, and dust storm days. The autumn to the following spring cumulative grassland fires (both days and burned area) affected the spring cumulative total dust weather days and dust storm days substantially, similar to the results of Yu and Ginoux [15]. In contrast, the effect of autumn to the following spring cumulative grassland fire (both days and burned area) on the spring cumulative dust storm days was more significant. The phenomena may be related to more windy weather in Dornod aimag. Grassland fires damage surface vegetation and expose the soil surface [14,15]. As the temperature rises, soil moisture evaporates, drying the soil out [49–51]. When strong winds occur, the wind sweeps up a large amount of dust on the exposed surface, and wind erosion will be enhanced with an increase in wind speed [52], causing reduced visibility [53], and making an area prone to dust storms. To enhance the credibility of the results, representative examples were selected from the analyzed data. The mechanisms of the effects of grassland fires on dust weather were explored in terms of precipitation, vegetation cover, grassland fires, dust-storm time series, and wind speed condition.

The present study had some limitations. Firstly, the data on grassland fire burned area were obtained from high-resolution satellite monitoring, while the dust data were derived from four ground observation stations within the study area. Given the disparity in data sources, we treated the study area as a whole and focused on the temporal correlation between grassland fires and dust weather. However, this approach did not adequately address the spatial correlation between the two. Therefore, future research should employ long-term series of high-resolution satellite dust data to more comprehensively explore the relationship between grassland fires and dust weather.

5. Conclusions

In the present study, Dornod aimag in Mongolia, a typical temperate grassland area, was selected as the study area to analyze the spatiotemporal characteristics of grassland fires and dust weather from 2001 to 2022, to evaluate the effect of grassland fires on dust weather, and to explore the mechanisms by which grassland fires affect dust weather. Grassland fires in Dornod aimag occurred mainly in spring, summer, and autumn, and dust weather was concentrated primarily in spring. Autumn to the following spring cumulative grassland fires (both days and burned area) significantly affected the spring cumulative dust weather

days, which were all positively correlated at the 0.01 level. In particular, it had a more significant effect on the spring cumulative dust storm days ($p = 0.0005$ and 0.001). Further analysis of the mechanisms of the effects of grassland fire on dust weather revealed that abundant summer precipitation resulted in higher vegetation cover and more accumulated fuels from autumn to April of the following spring. Consequently, cumulative grassland fire days were higher, and the cumulative burned area was larger during the period, leading to a significant increase in cumulative dust storm days in May of the spring. The findings can help us better understand the relationship between grassland fire and dust weather, which is essential for preventing and reducing grassland fires and dust storms. Moreover, they can provide an effective basis for developing desertification control strategies in the eastern steppe region of Mongolia.

Author Contributions: Conceptualization, L.W.; methodology, R.F. and E.J.; software, L.W. and E.J.; formal analysis, L.W.; resources, M.Y. and Y.B.; writing—original draft preparation, L.W.; writing—review and editing, L.W., M.Y., and Y.B.; visualization, L.W.; supervision, M.Y., Y.B., and R.F.; project administration, M.Y., Y.B., and R.F.; funding acquisition, M.Y. All authors have read and agreed to the published version of the manuscript.

Funding: This research was funded by the International (Regional) Cooperation and Exchange Program of the National Natural Science Foundation of China (Grant No. 42261144746), the Natural Science Foundation of Inner Mongolia Autonomous Region (Grant No. 2023LHMS04002), the Key R&D and Achievement Transformation Program of Inner Mongolia Autonomous Region (Grant No. 2022YFSH0091), and the Key scientific research projects and soft science research projects for military civilian integration in Inner Mongolia Autonomous Region (Grant No. JMRKX202207).

Data Availability Statement: The data source section of this study includes the original burned-area data and the SYNOP dust data download website. The generated data in the study are available from the corresponding author upon reasonable request.

Acknowledgments: We are grateful to the anonymous reviewers for their comments that have helped to improve the original manuscript. At the same time, we sincerely appreciate the generous support of our sponsors, whose financial contributions have allowed this paper to be successfully published.

Conflicts of Interest: The authors declare no conflict of interest.

Appendix A

Table A1. Correlation analysis between autumn to the following spring cumulative grassland fire (days and burned area) and the spring cumulative dust weather (total dust weather days and dust storm days).

	Autumn to the Following Spring Cumulative Grassland Fire Days	Autumn to the Following Spring Cumulative Burned Area
The spring cumulative total dust weather days	0.356 ***	0.295 ***
The spring cumulative dust storm days	0.376 ***	0.353 ***

*** indicates a significant correlation at the 0.01 level.

References

- Chen, J.; Wu, Y.; Wu, S.; Xie, L.; Tang, J.; Xu, Z.; Han, X.; Ma, X.; Zheng, W.; Sun, T.; et al. Application of FY-4B Geostationary Meteorological Satellite in Grassland Fire Dynamic Monitoring. *IEEE Trans. Geosci. Remote Sens.* **2023**, *61*, 1. [[CrossRef](#)]
- Zhang, R.P.; Zhou, J.H.; Guo, J.; Miao, Y.H.; Zhang, L.L. Inversion models of aboveground grassland biomass in Xinjiang based on multisource data. *Front. Plant Sci.* **2023**, *14*, 2. [[CrossRef](#)] [[PubMed](#)]
- Zhou, H.; Wang, Y.; Zhou, G. Temporal and spatial dynamics of grassland fires in Inner Mongolia. *Acta Prataculturae Sin.* **2016**, *25*, 16–25. [[CrossRef](#)]
- Qu, Z.; Zheng, S.; Bai, Y. Spatiotemporal patterns and driving factors of grassland fire on Mongolian Plateau. *Chin. J. Appl. Ecol.* **2010**, *21*, 807–813. [[CrossRef](#)]

5. Cao, H.; Fu, C.; Zhang, W.; Liu, J. Characterizing Sand and Dust Storms (SDS) Intensity in China Based on Meteorological Data. *Sustainability* **2018**, *10*, 2372. [[CrossRef](#)]
6. Bao, C.; Yong, M.; Bueh, C.; Bao, Y.; Jin, E.; Bao, Y.; Purevjav, G. Analyses of the Dust Storm Sources, Affected Areas, and Moving Paths in Mongolia and China in Early Spring. *Remote Sens.* **2022**, *14*, 3661. [[CrossRef](#)]
7. Shao, Y.; Klose, M.; Wyrwoll, K.-H. Recent global dust trend and connections to climate forcing. *J. Geophys. Res. Atmos.* **2013**, *118*, 2. [[CrossRef](#)]
8. Bao, C.; Yong, M.; Jin, E.; Bao, Y.; Tu, X.; Bao, Y. Regional spatial and temporal variation characteristics of dust in East Asia. *Geogr. Res.* **2021**, *40*, 3002–3015. [[CrossRef](#)]
9. Goudie, A.S. Desert dust and human health disorders. *Environ. Int.* **2014**, *63*, 101–113. [[CrossRef](#)]
10. Yu, S.; Jiang, L.; Du, W.; Zhao, J.; Zhang, H.; Zhang, Q.; Liu, H. Estimation and Spatio-temporal Patterns of Carbon Emissions from Grassland Fires in Inner Mongolia, China. *Chin. Geogr. Sci.* **2020**, *30*, 573. [[CrossRef](#)]
11. Ginoux, P.; Prospero, J.M.; Gill, T.E.; Hsu, N.C.; Zhao, M. Global-scale attribution of anthropogenic and natural dust sources and their emission rates based on MODIS Deep Blue aerosol products. *Rev. Geophys.* **2012**, *50*, 1–2. [[CrossRef](#)]
12. Rashki, A.; Kaskaoutis, D.G.; Sepehr, A. Statistical evaluation of the dust events at selected stations in Southwest Asia: From the Caspian Sea to the Arabian Sea. *Catena* **2018**, *165*, 590–591. [[CrossRef](#)]
13. Wang, Z.; Huang, R.; Yao, Q.; Zong, X.; Tian, X.; Zheng, B.; Trouet, V. Strong winds drive grassland fires in China. *Environ. Res. Lett.* **2023**, *18*, 015005. [[CrossRef](#)]
14. Idris, M.H.; Kuraji, K.; Suzuki, M. Evaluating vegetation recovery following large-scale forest fires in Borneo and northeastern China using multi-temporal NOAA/AVHRR images. *J. For. Res.* **2005**, *10*, 101–111. [[CrossRef](#)]
15. Yu, Y.; Ginoux, P. Enhanced dust emission following large wildfires due to vegetation disturbance. *Nat. Geosci.* **2022**, *15*, 878–883. [[CrossRef](#)]
16. Bao, C.; Yong, M.; Bi, L.; Gao, H.; Li, J.; Bao, Y. Impacts of Underlying Surface on the Dusty Weather in Central Inner Mongolian Steppe, China. *Earth Space Sci.* **2021**, *8*, 1–17. [[CrossRef](#)]
17. Sankey, J.B.; Germino, M.J.; Glenn, N.F. Relationships of post-fire aeolian transport to soil and atmospheric conditions. *Aeolian Res.* **2009**, *1*, 75. [[CrossRef](#)]
18. Whicker, J.J.; Breshears, D.D.; Wasiolek, P.T.; Kirchner, T.B.; Tavani, R.A.; Schoep, D.A.; Rodgers, J.C. Temporal and Spatial Variation of Episodic Wind Erosion in Unburned and Burned Semiarid Shrubland. *J. Environ. Qual.* **2002**, *31*, 599–612. [[CrossRef](#)]
19. Faustino-Eslava, D.V.; Yumul, G.P.; Servando, N.T.; Dimalanta, C.B. The January 2009 anomalous precipitation associated with the “Tail-end of the Cold Front” weather system in Northern and Eastern Mindanao (Philippines): Natural hazards, impacts and risk reductions. *Glob. Planet. Chang.* **2011**, *76*, 85–94. [[CrossRef](#)]
20. Wang, T.; Tu, X.; Singh, V.P.; Chen, X.; Lin, K.; Lai, R.; Zhou, Z. Socioeconomic drought analysis by standardized water supply and demand index under changing environment. *J. Clean. Prod.* **2022**, *347*, 131248. [[CrossRef](#)]
21. Xu, S.; Wu, Q.; Qiao, D.; Mu, Y.; Zhang, X.; Liu, Y.; Yang, X.; Shi, Z. Spatiotemporal pattern and effecting factors of wildfire in eastern Mongolia. *J. Desert Res.* **2021**, *41*, 83–91. [[CrossRef](#)]
22. Bao, T.; Gao, T.; Nandintsetseg, B.; Yong, M.; Jin, E. Variations in Frequency and Intensity of Dust Events Crossing the Mongolia–China Border. *Sola* **2021**, *17*, 147–149. [[CrossRef](#)]
23. Li, Y.; Zhao, J.; Guo, X.; Zhang, Z.; Tan, G.; Yang, J. The Influence of Land Use on the Grassland Fire Occurrence in the Northeastern Inner Mongolia Autonomous Region, China. *Sensors* **2017**, *17*, 437. [[CrossRef](#)] [[PubMed](#)]
24. Liu, M.; Zhao, J.; Guo, X.; Zhang, Z.; Tan, G.; Yang, J. Study on Climate and Grassland Fire in HulunBuir, Inner Mongolia Autonomous Region, China. *Sensors* **2017**, *17*, 616. [[CrossRef](#)]
25. Hope, A.; Tague, C.; Clark, R. Characterizing post-fire vegetation recovery of California chaparral using TM/ETM+ time-series data. *Int. J. Remote Sens.* **2007**, *28*, 1339–1354. [[CrossRef](#)]
26. Lacouture, D.L.; Broadbent, E.N.; Crandall, R.M. Detecting Vegetation Recovery after Fire in A Fire-Frequented Habitat Using Normalized Difference Vegetation Index (NDVI). *Forests* **2020**, *11*, 749. [[CrossRef](#)]
27. An, L.; Che, H.; Xue, M.; Zhang, T.; Wang, H.; Wang, Y.; Zhou, C.; Zhao, H.; Gui, K.; Zheng, Y.; et al. Temporal and spatial variations in sand and dust storm events in East Asia from 2007 to 2016: Relationships with surface conditions and climate change. *Sci Total Environ.* **2018**, *633*, 452–462. [[CrossRef](#)]
28. Bao, T.; Xi, G.; Deng, B.; Chang, I.S.; Wu, J.; Jin, E. Long-term variations in spatiotemporal clustering characteristics of dust events in potential dust sources in East Asia. *Catena* **2023**, *232*, 1–14. [[CrossRef](#)]
29. Gavrouzou, M.; Hatzianastassiou, N.; Gkikas, A.; Korras-Carraca, M.-B.; Mihalopoulos, N. A Global Climatology of Dust Aerosols Based on Satellite Data: Spatial, Seasonal and Inter-Annual Patterns over the Period 2005–2019. *Remote Sens.* **2021**, *13*, 359. [[CrossRef](#)]
30. Jugder, D.; Shinoda, M.; Sugimoto, N.; Matsui, I.; Nishikawa, M.; Park, S.-U.; Chun, Y.-S.; Park, M.-S. Spatial and temporal variations of dust concentrations in the Gobi Desert of Mongolia. *Glob. Planet. Chang.* **2011**, *78*, 14–22. [[CrossRef](#)]
31. Liu, X.; Song, H.; Lei, T.; Liu, P.; Xu, C.; Wang, D.; Yang, Z.; Xia, H.; Wang, T.; Zhao, H. Effects of natural and anthropogenic factors and their interactions on dust events in Northern China. *Catena* **2021**, *196*, 104919. [[CrossRef](#)]
32. Zhang, X.X.; Lei, J.Q.; Wu, S.X.; Li, S.Y.; Liu, L.Y.; Wang, Z.F.; Huang, S.Y.; Guo, Y.H.; Wang, Y.D.; Tang, X.; et al. Spatiotemporal evolution of aeolian dust in China: An insight into the synoptic records of 1984–2020 and nationwide practices to combat desertification. *Land Degrad. Dev.* **2023**, *34*, 2005–2023. [[CrossRef](#)]

33. Aryal, Y.; Evans, S. Dust emission response to precipitation and temperature anomalies under different climatic conditions. *Sci. Total Environ.* **2023**, *874*, 162335. [[CrossRef](#)] [[PubMed](#)]
34. Lee, E.-H.; Sohn, B.-J. Recent increasing trend in dust frequency over Mongolia and Inner Mongolia regions and its association with climate and surface condition change. *Atmos. Environ.* **2011**, *45*, 4611–4616. [[CrossRef](#)]
35. Li, Y.; Hu, X.; Wang, X.; Ji, M. Impact of transient eddy fluxes on the dust storm event: Cases study in South Xinjiang, China. *Atmos. Res.* **2022**, *269*, 106054. [[CrossRef](#)]
36. Liu, L.; Wang, D.; Wang, Z.; Zhong, J.; Zhang, Y.; Wu, R.; Zhang, X. Implications of North Atlantic warming for a possible increase of dust activity in northern East Asia. *Atmos. Res.* **2022**, *271*, 106092. [[CrossRef](#)]
37. Du, J.; Bao, G.; Tong, S.; Huang, X.; Wen, D.; Mei, L.; Bao, Y. Variations in vegetation cover and its relationship with climate change and human activities in Mongolia during the period 1982–2015. *Acta Prataculturae Sin.* **2021**, *30*, 9–11. [[CrossRef](#)]
38. Lai, Q. Simulation of GPP Based on Solar-induced Chlorophyll Fluorescence and its Response to Drought in Mongolian Plateau. Ph.D. Thesis, School of Environment, Northeast Normal University, Changchun, China, 2021.
39. Sun, H.; Wang, W.J.; Liu, Z.; Zou, X.; Zhang, Z.; Ying, H.; Dong, Y.; Yang, R. The relative importance of driving factors of wildfire occurrence across climatic gradients in the Inner Mongolia, China. *Ecol. Indic.* **2021**, *131*, 108249. [[CrossRef](#)]
40. Takemi, T. Dust storms and cyclone tracks over the arid regions in east Asia in spring. *J. Geophys. Res.* **2005**, *110*, 2. [[CrossRef](#)]
41. Wu, J.; Kurosaki, Y.; Shinoda, M.; Kai, K. Regional Characteristics of Recent Dust Occurrence and Its Controlling Factors in East Asia. *Sola* **2016**, *12*, 187–188. [[CrossRef](#)]
42. Na, L.; Zhang, J.; Bao, Y.; Bao, Y.; Na, R.; Tong, S.; Si, A. Himawari-8 Satellite Based Dynamic Monitoring of Grassland Fire in China-Mongolia Border Regions. *Sensors* **2018**, *18*, 276. [[CrossRef](#)] [[PubMed](#)]
43. Rihan, W.; Zhao, J.; Zhang, H.; Guo, X.; Ying, H.; Deng, G.; Li, H. Wildfires on the Mongolian Plateau: Identifying Drivers and Spatial Distributions to Predict Wildfire Probability. *Remote Sens.* **2019**, *11*, 2361. [[CrossRef](#)]
44. Bao, Y.; Shinoda, M.; Yi, K.; Fu, X.; Sun, L.; Nasanbat, E.; Li, N.; Xiang, H.; Yang, Y.; Davdaijavzmaa, B.; et al. Satellite-Based Analysis of Spatiotemporal Wildfire Pattern in the Mongolian Plateau. *Remote Sens.* **2022**, *15*, 190. [[CrossRef](#)]
45. Gerel, O.; Pirajno, F.; Batkhashig, B.; Dostal, J. *Mineral Resources of Mongolia*; Springer: Singapore, 2021; pp. 1–12.
46. Xu, J. Sand-dust storms in and around the Ordos Plateau of China as influenced by land use change and desertification. *Catena* **2006**, *65*, 279–284. [[CrossRef](#)]
47. Shen, Z.; Zhang, Q.; Chen, D.; Singh, V.P. Varying effects of mining development on ecological conditions and groundwater storage in dry region in Inner Mongolia of China. *J. Hydrol.* **2021**, *597*, 125759. [[CrossRef](#)]
48. Fan, B.; Guo, L.; Li, N.; Chen, J.; Lin, H.; Zhang, X.; Shen, M.; Rao, Y.; Wang, C.; Ma, L. Earlier vegetation green-up has reduced spring dust storms. *Sci. Rep.* **2014**, *4*, 2–5. [[CrossRef](#)]
49. Liu, Y.; Shi, F.; Liu, X.; Zhao, Z.; Jin, Y.; Zhan, Y.; Zhu, X.; Luo, W.; Zhang, W.; Sun, Y.; et al. Influence of Different Meteorological Factors on the Accuracy of Back Propagation Neural Network Simulation of Soil Moisture in China. *Sustainability* **2022**, *14*, 16381. [[CrossRef](#)]
50. Li, X.; Liu, L.; Li, H.; Wang, S.; Heng, J. Spatiotemporal soil moisture variations associated with hydro-meteorological factors over the Yarlung Zangbo River basin in Southeast Tibetan Plateau. *Int. J. Climatol.* **2019**, *40*, 199–202. [[CrossRef](#)]
51. Deng, Y.; Wang, S.; Bai, X.; Luo, G.; Wu, L.; Cao, Y.; Li, H.; Li, C.; Yang, Y.; Hu, Z.; et al. Variation trend of global soil moisture and its cause analysis. *Ecol. Indic.* **2020**, *110*, 5–9. [[CrossRef](#)]
52. Zhang, H.; Gao, Y.; Sun, D.; Liu, L.; Cui, Y.; Zhu, W. Wind Erosion Changes in a Semi-Arid Sandy Area, Inner Mongolia, China. *Sustainability* **2019**, *11*, 188. [[CrossRef](#)]
53. Tatarko, J.; van Donk, S.J.; Ascough, J.C., 2nd; Walker, D.G. Application of the WEPS and SWEEP models to non-agricultural disturbed lands. *Heliyon* **2016**, *2*, 2. [[CrossRef](#)] [[PubMed](#)]

Disclaimer/Publisher’s Note: The statements, opinions and data contained in all publications are solely those of the individual author(s) and contributor(s) and not of MDPI and/or the editor(s). MDPI and/or the editor(s) disclaim responsibility for any injury to people or property resulting from any ideas, methods, instructions or products referred to in the content.